
Article:
Bastir, Markus, García-Martínez, Daniel, Torres-Tamayo, Nicole et al. (5 more authors) (2017) In Vivo 3D Analysis of Thoracic Kinematics : Changes in Size and Shape During Breathing and Their Implications for Respiratory Function in Recent Humans and Fossil Hominins. Anatomical Record: Advances in Integrative Anatomy and Evolutionary Biology. pp. 255-264. ISSN 1932-8494

https://doi.org/10.1002/ar.23503

In vivo 3D analysis of thoracic kinematics: changes in size and shape during breathing and their implications for respiratory function in recent humans and fossil hominins

Markus Bastir[*1], Daniel García-Martínez[1,2], Nicole Torres-Tamayo[1], Juan Alberto Sanchis-Gimeno[3], Paul O'Higgins[4], Cristina Utrilla[5], Isabel Torres Sánchez[5], Francisco García Río[5]

[1] Paleoanthropology Group, Museo Nacional de Ciencias Naturales, CSIC, Madrid, Spain

[2] Science Faculty Autónoma University of Madrid, Spain

[3] Department of Anatomy and Human Embryology, Faculty of Medicine, University of Valencia, Spain

[4] Dept. of Archaeology and Hull York Medical School, The University of York, United Kingdom

[5] Hospital Universitario La Paz, Biomedical Research Institute (Idipaz), Madrid, Spain

[*] Corresponding author: Dr. Markus Bastir. Museo Nacional de Ciencias Naturales, CSIC, Calle JG Abascal 2, 28006 Madrid, Spain. Tel +34 91 566 8976, Fax 34 915668960; e-mail: mbastir@mncn.csic.es

Abstract

The human ribcage expands and contracts during respiration as a result of the interaction between the morphology of the ribs, the costo-vertebral articulations and respiratory muscles. Variations in these factors are said to produce differences in the kinematics of the upper thorax and the lower thorax, but the extent and nature of any such differences and their functional implications have not yet been quantified. Applying geometric morphometrics we measured 402 three-dimensional (3D) landmarks and semilandmarks of 3D models built from computed tomographic scans of thoraces of 20 healthy adult subjects in maximal forced inspiration (FI) and expiration (FE). We addressed the hypothesis that upper and lower parts of the ribcage differ in kinematics and compared different models of functional compartmentalization. During inspiration the thorax superior to the level of the sixth ribs undergoes antero-posterior expansion that differs significantly from the medio-lateral expansion characteristic of the thorax below this level. This supports previous suggestions for dividing the thorax into a pulmonary and diaphragmatic part. While both compartments differed significantly in mean size and shape during FE and FI the size changes in the lower compartment were significantly larger. Additionally, for the same degree of kinematic shape change, the pulmonary thorax changes less in size than the diaphragmatic thorax. Therefore, variations in the form and function of the diaphragmatic thorax will have a strong impact on respiratory function. This has important implications for interpreting differences in thorax shape in terms of respiratory functional differences within and among recent humans and fossil hominins.

1. Introduction

The human ribcage expands and contracts during breathing as a result of rib motion and the interaction between the curved ribs, their sternal connections, the anatomy and actions of the respiratory muscles and the ranges of movement at the costo-vertebral joints (Beyer et al., 2014; Ratnovsky et al., 2008). Two different patterns of ventilatory rib motion are commonly described, a "pump handle-like" movement of the upper ribs, and a "bucket handle-like" movement of the lower ribs (Beyer et al., 2014; Franciscus and Churchill, 2002; West 2012). Additionally, a "caliper-like" motion has been ascribed to the lowest two (Chila, 2010) or lowest five ribs (Magee, 2014). However, the impact of these movements on functional changes of the size and shape of the skeletal thorax during respiration are unclear.

So far, functional studies of thoracic breathing kinematics have focused mainly on external chest wall movements. These studies found that the diaphragm and the lower thorax contribute considerably more to changes in thoracic volume during breathing than the upper thorax (LoMauro et al*.,* 2012; Romei et al., 2010; Silvattia et al., 2012).

A recent *in vivo* 3D kinematic analysis of rib motion in the skeletal thorax suggested that the traditional dichotomy of "bucket handle" and "pump handle" rib rotations applies simultaneously to all levels (Beyer et al., 2014). But how do rib rotations contribute to differences in 3D size and shape changes of the entire thorax during breathing? What are the functional implications of kinematic shape changes of the thorax?

A given rib rotation will have a different effect on thoracic movement when carried out by flatter and straighter ribs than by more curved ribs with greater torsion. Consequently, because curvature and torsion differ among ribs of the upper and lower regions of the thorax (García Martínez et al., 2016), during inspiration the kinematic transformations experienced by these regions should also differ. This is not only important for breathing function in recent humans, but also in fossil hominins. Recent research and discoveries increasingly demonstrate the

enormous 3D variation in curvature, torsion and size of fossil hominin ribs (Gómez Olivencia et al. 2009; Schmid et al., 2013; García Martínez et al., 2014; Bastir et al., 2015; Berger et al., 2013, Tawane et al., 2016).

Consequently, there is a need to better understand the 3D kinematic changes in thoracic size and shape that occur during breathing in healthy subjects, and the functional significance of such variations. Such knowledge will be of use in relation to interpreting evolutionary transformations in rib size and shape in our own lineage and has the potential to be applicable in clinical contexts, e.g. lung disease, ribcage pathologies etc.

From a skeletal point of view, the ribs are conventionally classified into true ribs (1-7), false ribs (8-10) and floating ribs (11, 12) (Waldeyer and Mayet, 1987; Drake et al., 2010; White et al., 2011). Comparative ontogenetic study has also shown that growth trajectories of true ribs (1-7) are similar to each other, and differ from those of lower ribs (García-Martínez et al., 2016). However, within the non-floating ribs (ribs 1-10) recent studies (Bastir et al., 2013) have divided the thorax into an upper (ribs 1-5), and a lower unit (ribs 6-10). Additionally, it has been suggested that the first five thoracic vertebrae (T1-T5) and their costo-vertebral joints show a different pattern of serial morphological shape changes than the lower ones (T6-T10) (Bastir et al., 2014).

From a musculo-skeletal point of view, the thorax has been divided into a pulmonary ribcage (ribs 1-6) and diaphragmatic ribcage (ribs 7-12) (Ward et al., 1992; Kenyon et al., 1997). This is based on the apposition of the inner surface of the first six ribs to the lungs, and the attachment of the diaphragm to the lower six ribs (Ward et al., 1992). Muscle insertions further suggest such a compartimentalization: the scalenes, parasternal intercostals and the sternocleidomastoid muscles insert onto ribs 1-6, and the diaphragm arises from ribs 7-12 (Kenyon et al., 1997; De Troyer et al., 2005). Thus, the direct actions of the major extrinsic

respiratory muscles are almost exclusively on the pulmonary rib cage which differs regarding its movements from the diaphragmatic and abdominal part of the ribcage (Ward et al., 1992).

In this study we quantify in 3D, the kinematic changes among the parts of the thorax bounded by the first 10 ribs in healthy non-smoker subjects during breathing. We first explore the geometric shape changes during breathing kinematics in the full thorax and their relation to classical descriptions in terms of pump and bucket handle and caliper-like movements. We then examine the extent to which different modes and magnitudes of size and shape change exist among and within different regions of the upper and lower thorax during breathing.

2. Methods

2.1 Subjects

Thoracic computed tomography (CT) scans of 20 adult subjects (16 males, 4 females) in maximal forced inspiration (FI) and maximal forced expiration (FE) during the CT study were obtained from healthy non-smoker volunteers. Consistent with the Helsinki protocol (Goodyear et al. 2007) and in compliance with the stipulations of the local ethical committee, written consent was obtained to use these data for research purposes. Ages ranged from 40 to 67 years (average 50.9 years). Subjects presented an average total lung volume of 6.8l (sd. 1.19) and their average residual volume was 2.1l (sd. 0.45).

2.2. 3D-data

All CT examinations were performed with a 16-MDCT scanner (Somatom Sensation 16, Siemens Medical Solutions, Erlangen, Germany). Scanning voltage was 120 kV and current was 160 mA. CT of the thorax was performed from the lung apex to the level of the diaphragm in forced inspiration (FI) followed by forced expiration (FE). All imaging was performed with a collimation of 16 × 0.75 mm, table feed of 30 mm/rotation, and rotation time of 0.6 second/360° tube rotation with a standard reconstruction algorithm. CT capture lasted less than one minute. All

subjects were previously instructed how to correctly carry out FI and FE in order to minimize inter-individual variation in depth of breathing and so, size and shape changes in the thorax.

3D-surface meshes of upper and lower rib cages were extracted by MIMICS software (http://biomedical.materialise.com/mimics) from the CT data and a total of 402 landmarks and semilandmarks (Bastir et al., 2013) were placed using ViewBox 4 (www.dhal.com) software on these models: one landmark at the uppermost, one at the lowermost part of the articular surface of the rib head, and one at the anterior-most point on the intra-articular crest, two landmarks at the inferior and superior limits of the sternal extremity, one at the most lateral articular tubercle, and one at the inferior part of the costal angle. In addition, we measured 13 evenly spaced semilandmarks along the shaft of each rib and two landmarks at the manubrium (Supplementary Figure 1). Because CT-scanning was carried out to include the skeletal thorax to the level of the diaphragm, in many cases the 11^{th} and 12^{th} rib were not available for measurement. In consequence, we only took landmark coordinates on the non-floating ribs (1-10).

While landmarks characterize homologous anatomical structures as points (Oxnard and O´Higgins, 2009), curve semilandmarks respect homology at a different level. Rather than the (semi)landmark itself, the curve in total (i.e. the rib shaft) is considered biologically comparable (Gunz and Mitteroecker, 2013). Semilandmarks were slid twice, the first time to the template specimen (the first specimen in the sample) and after sliding of all specimens against the common mean shape they were slid again to the overall mean, so as to minimize the bending energy between each ribcage and this mean (Gunz and Mitteroecker , 2013). This sliding manoeuvre minimizes variation due to error in siting of semilandmarks along the curve.

2.3 Geometric morphometric analyses

The 3D coordinates were subjected to a Generalized Procrustes analysis (GPA) that applies translation, scaling and rotation to the landmark coordinates to produce Procrustes shape

coordinates (O'Higgins, 2000). Shape differences are quantified by Procrustes distance (*Pd*, the summed, squared interlandmark distances between corresponding landmarks) (O'Higgins, 2000; Gunz and Mitteroecker, 2013). Size is measured as Centroid size (CS), the summed squared distances between each landmark and the centre of the full landmark configuration.

Centroid size is extracted as a scaling factor that emerges during GPA when all landmark configurations are standardised to unit size (O'Higgins, 2000; Gunz and Mitteroecker 2013). Shape data were corrected for sexual dimorphism by multivariate regression of shape on sex-dummy variables because of unbalanced sex sampling similar to a MANCOVA approach (Rosas and Bastir, 2002). Asymmetries were removed by computing the mean of each thoracic landmark configuration and its reflection after GPA (Bastir et al*.,* 2013).

Kinematic differences in ribcage shape were assessed by regression of shape on kinematic status (forced expiration/ forced inspiration) and mean shape comparisons. A permutation test (N=10000) with permuted kinematic status was used to estimate the statistical significance of the observed shape difference (Klingenberg, 2011). The differences between mean inspiratory and expiratory ribcage shapes were visualized using transformation grids calculated using a triplet of thin plate splines (TPS). TPS-grids were positioned in the coronal and sagittal plane (red grids) and in two transverse planes, one within the upper (green grid), and the other within the lower thorax (orange grid). Warpings of the grids were computed between the overall mean shape (reference) and the mean shapes at FI and FE.

In order to identify differences in rib kinematics among regions of the thorax we assessed the significance of apparent differences among adjacent pairs of ribs. Thus, we compared shape changes occurring in the portion of the thorax bounded by rib pairs 1-2 with that bounded by rib pairs 2-3. This was repeated for ribs 3-4 vs 4-5, and so on until rib pair 9-10. Since each pair is represented by an equivalent set of landmarks we were able to directly perform GPA and subsequent statistical analyses. These comparisons allowed us to assess the validity in terms of

function of subdivision of the thorax into two regions. Thus, the regions enclosed by ribs 1-5 and 6-10, have previously employed by us based on vertebral geometry and for convenience (equivalent sets of landmarks) of morphometric analysis (Bastir et al., 2013; 2014), while regions enclosed by ribs 1-6 and 7-10 have been proposed to reflect the functional split between pulmonary and diaphragmatic divisions (Ward et al., 1992, Kenyon et al., 1997). Regions enclosed by ribs 1-7 and 8-10 have been differentiated by other workers based on skeletal anatomical criteria distinguishing between true and false ribs and on the basis of their ontogenetic trajectories (Waldeyer and Mayet, 1987; White et al., 2011; García Martínez et al., 2016).

Regression of the shapes of each partial thoracic region (rib pair) on kinematic status (forced inspiration, forced expiration) produced one kinematic vector connecting mean inspiratory and mean expiratory shape for each region of the thorax (or rib pair) and provided information on the magnitude of shape change due to breathing in the upper and lower thorax region (or rib pair). To compare these vectors among successive pairs of ribs, the angle between them was calculated. Its significance was estimated using a closed-form formula (Li, 2011) implemented in Morpho-J (Klingenberg , 2011; Klingenberg and Marugán-Lobón, 2013). Small angles indicate roughly parallel kinematic vectors (similar shape change during breathing), while greater angles indicate divergent vectors (different breathing kinematics).

Functional size, that is, the differences in centroid size (CS) and between the inspiratory and expiratory configurations of upper and lower thoracic regions was used to test the hypothesis of different kinematic size changes of the upper and lower thoracic compartments during breathing. Functional shape is defined as the shape difference, measured as Procrustes distance, between thorax shape at FI and FE and used to test the hypothesis of different kinematic shape changes of the upper and lower thoracic compartments during breathing. Mean size and shape differences between inspiration and expiration, and between upper and

lower compartments, were compared using a paired t-test, with normality of the differences in CS and the Procrustes shape distances having been confirmed beforehand by the Kolmogorov Smirnov test (Sokal and Rohlf, 1998). Reduced major axis regressions were used to compare scaling relationships of kinematic differences in CS (functional size) and shape (Pd, functional shape) in the upper and lower thorax (Sokal and Rohlf, 1998).

3. Results

3.1. Mean shape comparisons of full rib cage

Permutation tests (1000 permutations) indicated significant differences in mean shapes (*Pd*=0.055; p<0.004) between whole ribcages in inspiration and expiration. The associated TPS-transformation grids of Figure 1 are shown in frontal, left lateral and cranial axial views. Frontal views show that the lateral (midshaft) part of the ribs becomes elevated relative to the spine throughout the entire ribcage. While the upper thorax expands antero-posteriorly the lower thorax expands medio-laterally from the 6^{th} and 7^{th} ribs onwards. There is no mediolateral expansion at the upper part of the thorax. The arrows drawn at the sternal ends of the fourth and eight ribs show this differential medio-lateral expansion. In addition, cranial, axial views illustrate that during inspiration the upper thorax increases in relative antero-posterior dimensions (green TPS grid), while the lower thorax shows a small increase in relative width (orange TPS grid). Thus, upper and lower parts of the thorax appear to deform differently during breathing.

3.2. Kinematic vector angle between adjacent rib pairs

Table 1 presents the associated regression results and tabulates the angles. The angles at rib level 2 and rib level 6 are slightly larger than at other levels indicating kinematic changes. This suggests that, from a functional point of view, the thorax can be divided into the thoracic aperture (1^{st} and 2^{nd} rib level), a region superior to the 6^{th} rib and a region inferior to the 6^{th} rib.

These latter results are compatible with a division of the ribcage according to kinematics into a pulmonary and a diaphragmatic part following musculo-skeletal criteria (Ward et al., 1992, Kenyon et al., 1997). The slight increase in angle at the level 5 may indicate action of the rectus abdominis muscle.

3.3. Pulmonary and diaphragmatic ribcage compartments

When the results of the previous analyses (Table 1) are taken as basis for a division of the ribcage into an upper and lower part, kinematic vector comparisons of the pulmonary and diaphragmatic thoracic regions lend quantitative support to apparent visual differences (Fig. 1). Mean shapes at FI and FE were different both in the pulmonary ($Pd=0.046$; $p<0.001$) and the diaphragmatic thorax ($Pd=0.035$; $p<0.05$). Mean centroid sizes (CS) at FE ($CS = 1517.2$) and at FI ($CS = 1529.8$) within the pulmonary ribcage also differed significantly ($t= -7.892$, $p<0.0001$). Within the diaphragmatic ribcage mean centroid sizes at FE ($CS= 1628$) and at FI ($CS= 1662.5$) differed also significantly ($t = -7.596$, $p<0.0001$). The angle between the pulmonary and diaphragmatic kinematic vectors was 36.6 degrees ($p<0.0001$) indicating different breathing kinematics.

3.4. Magnitudes of kinematic size and shape differences

Differences in CS between expiration and inspiration (functional size) were significantly greater in the diaphragmatic thorax (34.47) than the pulmonary thorax (12.62). Normality was not rejected by the Kolmogorov-Smirnov test ($d=0.1$; ns) and the paired t-test finds a statistical difference ($t=-4.54$, $p<0.01$).

For the pulmonary thorax the Procrustes distance between mean inspiratory and expiratory shapes (functional shape) is 0.053, and for the diaphragmatic, 0.046. Normality was not rejected by the Kolmogorov-Smirnov test ($d=0.20$; n.s.) and a paired t-test indicates no differences in Procrustes distances ($t=1.07$, n.s) (Table 2).

Thus, the pulmonary thorax produced less size difference during inspiration than the diaphragmatic part of the ribcage with similar amounts of deformation in shape. This is also seen in the regression analyses (Fig. 2, Table 3). The slope of the regression of functional size on functional shape or the pulmonary thorax is significantly smaller than that for the diaphragmatic, indicating that it needs to deform significantly more than the diaphragmatic thorax to produce the same size difference. Additionally, the functional size of the pulmonary thorax is only weakly related to functional size of the diaphragmatic thorax, while functional shapes of both thorax compartments are very highly correlated (Table 3).

4. Discussion

This study explored the geometric shape changes during breathing in the full thorax in adult healthy non-smoker subjects. We addressed the relationship of these shape changes to classical descriptions of rib motion in terms of pump and bucket handle and caliper-like movements (Beyer et al*.,* 2014; Ratnovsky et al*.,* 2008; West, 2012). We also investigated the basic functional implications of kinematic size and shape changes of the upper and lower thoracic compartments and assess our findings in an evolutionary morphological and clinical context.

4.1. Kinematic deformations, rib rotations and morpho-functional divisions

In recent and fossil hominins there is substantial variation in the size and shape of the upper and lower thorax (Schmid et al., 2013; Garcia Martínez et al., 2014; Bastir et al., 2015) with potential implications for breathing. In fact, upper and lower parts of the ribcage have been proposed to evolve (Schmid et al., 2013) and develop (Bastir et al., 2013, García Martínez et al., 2016) relatively independently. Various propositions as to how to divide the ribcage into an upper and lower compartment have been made following statistical, musculo-skeletal and purely skeletal criteria (Bastir et al., 2013, 2014, Ward et al., 1992, White et al., 2011, García Martínez et al., 2016). Our results suggest from a kinematic point of view a musculo-skeletal division of the thorax into a pulmonary part (ribs 3-6) and a diaphragmatic or abdominal part

(ribs 7-10) according to Ward et al. (1992) and Kenyon et al. (1997) who proposed such divisions on the basis of muscle insertions and contact between the ribs and lungs.

Table 1 also provides evidence for specific kinematic changes at the upper thoracic aperture (ribs 1 and 2). This has not previously been observed and may indicate the action of the accessory respiratory muscles - scalene muscles- necessary in forced inspiration. The flatness of ribs 1 and 2 compared to the torsion of mid-thoracic and lower ones (Mann, 1993; Dudar, 1993; Garcia Martínez et al., 2015) and the supine posture in the CT-scanner (Romei et al., 2010) may well reflect the specific kinematics of this region as indicated by the higher angle (Table 1).

The significant and large angle (36.6 degrees, $P<0.0001$) between pulmonary and diaphragmatic kinematic vectors together with the differences in transformation grid deformations between upper and lower thoracic regions (Fig. 1) provide clear evidence for different modes of deformation of the upper and lower parts of the breathing thorax.

The shape changes observed in the thorax do not completely reflect the oversimplification that "pump handle like" motions of the ribs characterize the upper thorax, and "bucket handle like" motions, the lower (Chila, 2010; Magee, 2014; West, 2012). In part this is because these terms are ill defined and so, are difficult to relate to a quantitative analysis of 3D motion, and in part because both motions are evident to some degree throughout the thorax (Beyer et al., 2014). This may account for the limited variation in kinematic angles among rib pairs (Table 1.). Also a third motion, caliper-like spreading apart of the anterior ends of the lower ribs (Chila, 2010; Magee, 2014) is observed in Figure 1. Rib shape and costosternal joints likely constrain these motions leading to pump-handle and caliper like motion in these lower parts increasing the distance between the anterior ends of the ribs of the diaphragmatic thorax. This caliper-like motion is not, as is commonly stated (Chila, 2010), restricted to the last two 'floating ribs' but affects all lower ribs to some degree, supporting Magee (2014). This caliper-like motion may

also reflect active muscle force during forced expiration because of the abdominal muscles insertions.

Respiratory movements of the thoracic cage are produced by the cumulative effects of small movements of the ribs at each costovertebral joint (Ward and Macklem, 1985). The axes of movement are complex and, particularly, those of the lower ribs are not well understood (Beyer et al., 2014). Moreover, these axes change in cranio-caudally as the transverse processes become increasingly posteriorly orientated (Latimer and Ward, 1993; Bastir et al., 2014) with kinematic consequences for thoracic shape changes during breathing. Regional differences in kinematic patterns shown in Figure 2 may reflect the successive changes in the articular surfaces, rib axes, and attachments. The upper ribs hinge about an axis running along their neck, their convex tubercle rotating within the concavity of the costo-transverse joint. In inspiration, the ribs become more horizontal. Their anterior end moves forwards and upwards, but only slightly laterally due to costosternal constraints. This results in anteroposterior expansion of the thoracic cavity and elevates the thoracic cage anteriorly (Fig. 1) (Agostini and Dángelo, 1985).

Because of the increasingly posteriorward sweep of the transverse processes, and so, of the axes of the necks of the ribs (Bastir et al., 2014), their anterior ends become progressively more laterally orientated in inspiration (Agostini and Dángelo, 1985), as is observed in Figure 1. Because the ribs increase cranio-caudally in length and curvature, upward rotation during inspiration shifts the ribs around the thorax at any given horizontal plane (Agostini and Dángelo, 1985; Mead et al., 1985). Moreover, the movement of the lower ribs includes a slight degree of eversion, which elevates the most lateral part of the rib shaft relative to a plane passing through its head posteriorly and the anterior end of its costal cartilage, anteriorly (Agostini and Dángelo, 1985).

In the lower thorax the shape and inclination of the costotransverse articular facets also allows for a gliding component (Ward and Macklem, 1985). In deep inspiration, the rib tubercles glide poseriorly, superiorly, and medially, swinging the anterior ends of the ribs horizontally laterally, away from each other (Ward and Macklem, 1985; Agostini and Dángelo, 1985; Mead et al., 1985). This further contributes to transverse expansion of the lower chest (Fig. 1a).

4.2. Functional and evolutionary anatomy

The breathing kinematics of the upper thorax produce a smaller functional size difference than in the lower thorax (Table 2, Fig. 2). There is also evidence that size changes in the upper and lower thorax are weakly correlated (Table 3). This weak correlation may reflect variation among subjects in breathing preferences with some being predominantly thoracic breathers and others, diaphragmatic breathers. This requires further investigation, however, recent work on sexual dimorphism suggests that the form of the lungs (Torres Tamayo et al., 2016) and that of the ribcage (Bellemare et al., 2003, 2006; Garcia Martínez et al, in revision) correlate with differences in respiratory function. Thus, females, who tend to show more prismatic (barrel shaped) thoraces also show reduced expansion capacities when compared to more pyramidal (funnel) shaped males (Bellemare et al., 2003; Romei et al., 2010; Layton et al., 2011). Variations related to skeletal aging might also contribute to the weak relationship between the functional sizes of the upper and lower parts of the thorax because aging leads to increased ossification in the costo-sternal cartilages and this, in turn, limits upper thoracic mobility (Oskvig, 1999; Gayzik et al. 2008).

The finding of a greater overall contribution to functional thorax size changes of the lower thorax is consistent with studies on external chest wall kinematics that have shown greater volumetric differences in the lower part of the chest than in the (upper) thoracic part (LoMauro et al., 2012; Romei et al., 2010; Silvattia et al., 2012). Because the diaphragm and its movements are not considered in our study, it is likely that changes in size of the upper skeletal

thorax with breathing more directly reflect lung volumetric changes than those of the lower skeletal thorax, although the latter are functionally more relevant than the former.

Frontal and lateral views in Figure 1 (and supplementary Movie 1) show that the rib rotations described by Beyer et al. (2014) lead to different costosternal motions in the upper thorax than in the lower. Thus, the costosternal joints of the upper ribs deform less than those of the lower, possibly as a consequence of differences in the lengths and orientations of the costosternal cartilages (Fig. 1). Thus, short and horizontally aligned cartilages are likely to permit smaller changes in thoracic width than longer and more caudally oriented costosternal cartilages. This costosternal constraint may also be reflected in the results of the regression analyses (Table 3), where the smaller slope in the pulmonary thorax indicates that for the same amount of size change, the upper thorax needs to change shape much more than the lower during breathing (Fig. 2). The reduced curvature and torsion of the upper ribs also contributes to smaller volumetric differences. Thus, greater curvature, torsion and lateral extension of the midshaft in shallow rib cages produce greater size differences between inspiration and expiration than in deep rib cages with less curved upper ribs. We have shown elsewhere that this mode of rib shape variation is a feature of normal variation, rather than pathological (Bastir et al., 2015, García Martínez et al., 2016).

The larger lower ribs enhance the degree of expansion of the lower rib cage during breathing (Table 2). As noted above, a recent study on modern human sexual dimorphism demonstrates a larger and relatively wider lower thorax in males combined with a significantly greater expansion capacity when compared to females (Garcia Martínez et al. in revision). The present findings with respect to how kinematic size and shape changes of upper and lower thoraces relate to rib and thorax shape are consistent with this, in that a wider thorax is expected to show greater volumetric changes during breathing. Further, the larger sizes of the mid- and lower thoracic ribs relative to the upper ribs in fossil hominins, such as Neandertals (García

Martínez et al., 2014; Bastir et al., 2015) and *Australopithecus* (Schmid et al., 2013, Tawane et al., 2016) can be expected to have important implications for breathing kinematics in these hominins, and so potentially contribute to better understanding of the energy demands and behaviours of our fossil relatives . This is a topic to be explored in future work.

4.3. Clinical implications

This study has focused on healthy subjects but the findings are of relevance to future research in pathological subjects. Thus, Chronic Obstructive Pulmonary Disease (COPD) results in pulmonary hyperinflation and respiratory muscle dysfunction (O'Donnell, 2001, Bellemare et al., 2001). Muscle dysfunction is characterized by changes in mechanical advantages and alterations of muscle fibre lengths, and intrinsic muscle structure (Marchand and Decramer, 2000). The diaphragm shows a flatter dome configuration, and loses its capacity to further expand the lower thorax (Marini, 1998). In consequence, the intercostal muscles become critical for inspiratory flow generation in these patients.

Such changes in respiratory muscles likely directly affect the kinematics of the upper and lower ribcage and these are further impacted by changes in the diaphragm that result in decreased lower chest expansion. Changes in ribcage kinematics in COPD impact lung expansion with consequences for the ventilation/perfusion ratio. Indeed, recent work shows that lung morphology and kinematics differ between COPD patients and healthy controls (Torres-Tamayo et al., 2015). The regional kinematic differences shown here (Figs. 1, 2; Table 2) are likely important in the light of mismatching between ventilation and flow, the commonest cause of hypoxemia in lung diseases (Kent et al., 2011). As such, it will be of interest to apply the methods used in the present study to a comparison of the breathing kinematics of upper and lower thoracic compartments among COPD patients and healthy subjects.

Alveolar recruitment, that is, opening of alveoli that remain closed during breathing at low lung volumes, can be a compensatory mechanism to minimize the consequences of gas exchange

imbalance (Rodríguez-Roisin and Wagner, 1990; West, 1990; Engel and Paiva, 1981). The lateral displacement of the lower thorax observed in this study (Fig. 1a,c) likely favors increased lung expansion during inspiration and, consequently, may be a key mechanical mechanisms underlying alveolar recruitment, with significant clinical implications in asthma and chronic bronchitis (Palmer et al., 1967).

Age is another factor that impacts breathing kinematics as alveolar recruitment will decrease with aging and its associated clinical problems (Oskvig, 1999). This is because as we age the ribs come to lie more horizontally. This is illustrated for the lower ribs by Weaver et al. (2014). Further with increasing age comes increasing thoracic kyphosis (Gayzik et al., 2008). This further impacts rib orientation, which reduces respiratory muscle strength, one of the most important physiological changes in the respiratory system associated with aging (Janssens et al., 1999). With age, joints become stiffer and less flexible and ribcage calcification extends from the costochondral junctions to the sternocostal junctions (Ontell et al., 1997). The resulting stiffening of ribcages in older subjects compromises their respiratory biomechanics, leading to "hyperinflation", with possible clinical effects similar to those of COPD patients. The approaches we have applied in the present study may well have application in future clinical assessment of these age changes.

Other potential applications include assessment of the progress and effects of thoracic and spinal skeletal dysplasias and of progressive thoracic skeletal deformities such as occur in *Osteogenesis imperfecta*. In fact, in a recent study of chest wall motion in Type III *Osteogenesis imperfecta* patients, asynchronies between upper and lower thorax kinematics were reported (LoMauro et al., 2012). These authors related these asynchronies to the presence of more horizontally aligned ribs. Figure 1 shows clearly that inspiratory expansion of the upper thorax occurs in the antero-posterior direction facilitated by kinematic elevation of upper ribs.

Therefore, disease leading to more horizontal upper ribs will also likely lead to clinical problems related to ventilation.

In this study we assessed the size and shape changes that occur in the upper and lower skeletal thorax during breathing by means of CT. This provides different insights into breathing mechanics than those that arise from the more usual studies of the diaphragm and intercostal muscle function (Romei et al., 2010; LoMauro et al., 2012; Silvattia et al., 2012) because breathing also involves the actions of the serratus, scalene, pectoral and abdominal wall muscles (Drake et al., 2010; Thibodeau and Patton, 2008; White et al., 2011). While CT studies cannot reveal respiratory muscle morphology and functioning during breathing they can potentially reveal the changes in function that arise as a consequence of muscular changes. Future research examining breathing kinematics using could be complemented by magnetic resonance imaging and electromyography to allow integration of data on muscle functioning with data on thorax motion.

5. Conclusions

Our study shows that the pulmonary and diaphragmatic parts of the thorax differ in terms of breathing kinematics, particularly in their modes of shape change during breathing while the degree of shape change is similar in both compartments. In contrast, the diaphragmatic part undergoes greater changes in size than the pulmonary part. In consequence a greater degree of deformation of the upper thorax is required to produce a similar degree of size change to that of the lower thorax. This has important implications with regard to the functional impact of variations in rib cage form among living and fossil hominins. The approaches employed in this study have potential clinical applications in assessing the impact and progress of the effects of disease and aging on breathing kinematics.

Acknowledgments We thank Nick Milne for discussions. Funding: Spanish Ministry of Economy and Competitiveness (CGL2012-37279, CGL2015-63648-P; MINECO), the Leakey Foundation, and PI10/02089 (Fondo de Investigación Sanitaria) Ministry of Health, Spain.

Literature cited

Agostini E. Dángelo E. 1985. Statics of the chest wall. In: The Thorax. Roussos CJ, Macklem PT, eds. New York: Marcel Dekker Inc. 259-295.

Bastir M, García-Martínez D, Recheis W, Barash A, Coquerelle M, Rios L. Peña-Melián Á. García Río F. O'Higgins P. 2013. Differential Growth and Development of the Upper and Lower Human Thorax. PLoS ONE 8, e75128.

Bastir M, García-Martínez D, Estalrrich A, Tabernero AG, Huguet R, Ríos L, Barash A, Recheis W, Rasilla MDI, Rosas A. 2015. The relevance of the first ribs of the El Sidrón site (Asturias, Spain) for the understanding of the Neanderthal thorax. J Hum Evol 80,64-73

Bastir M, Higuero A, Ríos L, García-Martínez D. 2014. Three-dimensional analysis of sexual dimorphism in human thoracic vertebrae: Implications for the respiratory system and spine morphology. Am J Phys Anthropol 155, 513-521.

Berger LR. 2013. The Mosaic Nature of Australopithecus sediba. Science 340(6129):163-165.

Berger LR, Hawks J, de Ruiter DJ, Churchill SE, Schmid P, Delezene LK, Kivell TL, Garvin HM, Williams SA, DeSilva JM et al. . 2015. Homo naledi, a new species of the genus Homo from the Dinaledi Chamber, South Africa. eLife 4.

Bellemare J-Fo, Cordeau M-P, Leblanc P, and Bellemare Fo. 2001. Thoracic dimensions at maximum lung inflation in normal subjects and in patients with obstructive and restrictive lung diseases. Chest 119(2):376-386.

Bellemare, F., Jeanneret, A., Couture, J., 2003. Sex differences in thoracic dimensions and configuration. American Journal of Respiratory and Critical Care Medicine 168, 305-312.

Bellemare, F., Fuamba, T., Bourgeault, A., 2006. Sexual dimorphism of human ribs. Respiratory Physiology and Neurobiology 150, 233-239.

Beyer B, Sholukha V, Dugailly PM, Rooze M, Moiseev F, Feipel V, Van Sint Jan S. 2014. In vivo thorax 3D modelling from costovertebral joint complex kinematics. Clin Biomech 29: 434-438.

Chila A. 2010. Foundations of Osteopathic Medicine. 3 ed. Philadelphia : Lippincott Williams & Wilkins.

De Troyer A, Kirkwood PA, Wilson TA. 2005. Respiratory Action of the Intercostal Muscles. Physiol Rev 85:717-756.

Drake RL, Wayne-Vogel A, Mitchell AWM (Eds.) 2010. Gray's anatomy. 2nd ed. Barcelona: Elsevier. p 124-158.

Dudar CJ.1993. Identification of Rib Number and Assessment of Intercostal Variation at the Sternal Rib End. J For Sci 38:788-797.

Engel LA, Paiva M. 1981. Analysis of the sequential filling and emptying of the lung. Resp Physiol 45:309-321.

Franciscus RG, Churchill SE. 2002. The costal skeleton of Shanidar 3 and a reappraisal of Neandertal thoracic morphology. J Hum Evol 42:303-356.

García-Martínez D, Barash A, Recheis W, Utrilla C, Torres Sánchez I, García Río F, Bastir M. 2014. On the chest size of Kebara 2. J Hum Evol 70:69-72.

García Martínez, D., Recheis, W., Bastir, M., 2016. The 3D variation of human rib curvature along ontogeny and its importance for the understanding of the thorax development. Am J Phys Anthropol 159: 423-431

García-Martínez D, Torres-Tamayo N, Torres-Sanchez I, García-Río F, and Bastir M. in revision. Morphological and functional implications of sexual dimorphism in the human skeletal thorax. Am J Phys Anthropol.

Tawane G, García-Martínez D, Eyre J, Bastir M, Berger L, Nalla S, and Williams SA. 2016. A hominin first rib discovered at the Sterkfontein Caves, South Africa. South African Journal of Science 112(5/6).

Gayzik FS, Yu MM, Danelson, KA, Slice DE, Stitzel JD. 2008. Quantification of age-related shape change of the human ribcage through geometric morphometrics. J Biomech 41:1545-1554.

Gómez-Olivencia A, Eaves-Johnson KL, Franciscus RG, Carretero JM, Arsuaga JL. 2009. Kebara 2: new insights regarding the most complete Neandertal thorax. J Hum Evol 57:75-90.

Goodyear MDE, Krleza-Jeric K, Lemmens T. 2007. The Declaration of Helsinki. BMJ 335:624-625.

Gunz P, and Mitteroecker P. 2013. Semilandmarks: a method for quantifying curves and surfaces. Hystrix 24(1):103-109.

Hostettler S, Illi SK, Mohler E, Aliverti A, Spengler, CM. 2011. Chest wall volume changes during inspiratory loaded breathing. Resp Phsyiol Neurol 175:130-139.

Janssens JP, Pache JC, Nicod LP. 1999. Physiological changes in respiratory function associated with aging. Eur Respir J 13:197-205

Jellema LM, Latimer, B, Walker A. 1993. The rib cage, The Nariokotome Homo Erectus Skeleton. Cambridge:Harvard University Press. p 294-325.

Kent BD, Mitchell PD, McNicholas WT. 2011. Hypoxemia in patients with COPD: cause, effects, and disease progression. Int J Chron Obstruct Pulmon Dis 6:199-208.

Kenyon CM, Cala SJ, Yan S, Aliverti A, Scano G, Duranti R, Pedotti A, and Macklem PT. 1997. Rib cage mechanics during quiet breathing and exercise in humans. Journal of Applied Physiology 83(4):1242-1255.

Klingenberg CP. 2011. MorphoJ: an integrated software package for geometric morphometrics. Mol Ecol Res 11:353-357.

Klingenberg CP, Marugán-Lobón J. 2013. Evolutionary Covariation in Geometric Morphometric Data: Analyzing Integration, Modularity and Allometry in a Phylogenetic Context. Syst Biol 62:591–610.

Latimer, B., Ward, C.V., 1993. The thoracic and lumbar vertebrae, The Nariokotome Homo Erectus Skeleton. Harvard University Press, Cambridge, pp. 266-293.

Layton AM, Garber CE, Thomashow BM, Gerardo RE, Emmert-Aronson BO, Armstrong HF, Basner RC, Jellen P, Bartels MN. 2011. Exercise ventilatory kinematics in endurance trained and untrained men and women. Resp Physiol Neurol 178:223-229.

Li, S. 2011. "Concise formulas for the area and volume of a hyperspherical cap." Asian J. Math. Statist. 4:66-70.

LoMauro A, Pochintesta S, Romei M, D'Angelo MG, Pedotti A, Turconi AC, Aliverti A. 2012. Ribcage Deformities Alter Respiratory Muscle Action and Chest Wall Function in Patients with Severe Osteogenesis Imperfecta. PLoS ONE 7, e35965.

Magee DJ. 2014. Orthopedic Physical Assessment. 6th ed. Saunders Elsevier.

Mann RW, 1993. A Method for Siding and Sequencing Human Ribs. J For Sci 38:151-155.

Marchand E, Decramer M. 2000. Respiratory muscle function and drive in chronic obstructive pulmonary disease. Clin Chest Med 21:679-92

Marini JJ, 1998. Dynamic hyperinflation. In: Physiological basis of ventilatory support. Marini, KK and Alutsky AS (eds). Marcel Dekker. New York p 453-90.

Mead J, Smith JC, Loring SJ.1985. Volume displacements of the chest wall and their mechanical significance. In: The Thorax. Roussos CJ, Macklem PT, (eds). New York: Marcel Dekker Inc 369-392.

O'Donnell DE. 2001. Assessment of bronchodilator efficacy in symptomatic COPD: is spirometry useful? Chest 117: 42S-7S.

O'Higgins P. 2000. The study of morphological variation in the hominid fossil record: biology, landmarks and geometry. J Anat 197:103-120.

Ontell FK, Moore EH, Shepard JA, Shelton DK. 1997. The costalcartilage in health and disease. RadioGraphics 17:571–577.

Oskvig, R.M., 1999. Special Problems in the Elderly. CHEST Journal 115, 158S-164S.

Oxnard C, and O'Higgins P. 2009. Biology Clearly Needs Morphometrics. Does Morphometrics Need Biology? Biological Theory 4(1):84-97.

Palmer KN, Diament ML. 1967. Spirometry and blood-gas tensions in bronchial asthma and chronic bronchitis. Lancet. Aug 19; 2(7512):383–384

Ratnovsky A, Elad D, Halpern P. 2008. Mechanics of respiratory muscles. Resp. Physiol Neurol 163:82-89.

Rodríguez-Roisin R, Wagner PD. 1990. Clinical relevance of ventilation-perfusion inequality determined by inert gas elimination. Eur Respir J 3: 469-482.

Romei M, Mauro AL, D'Angelo MG, Turconi AC, Bresolin N, Pedotti A, Aliverti, A. 2010. Effects of gender and posture on thoraco-abdominal kinematics during quiet breathing in healthy adults. Resp Physiol Neurol 172:184-191.

Schmid P, Churchill SE, Nalla S, Weissen E, Carlson KJ, de Ruiter DJ, Berger LR. 2013. Mosaic Morphology in the Thorax of Australopithecus sediba. Science 340.

Silvattia AP, Sarrob KJ, Cerveric P, Baronic G, Barrosa RML. 2012. A 3D kinematic analysis of breathing patterns in competitive swimmers. J Sport Sci 30:1551-1560.

Sokal RR, Rohlf FJ. 1998. Biometry. 3 ed. New York : W. H. Freeman and Company.

Thibodeau GA, Patton KT. 2008. Structure and function of the body. 13nd ed. Barcelona, Elsevier.

Torres-Tamayo SN, García-Martínez D, Bastir M, Utrilla C, Torres Sánchez I, García Río F. 2015. Estudio de la morfología pulmonar en pacientes con EPOC, y su influencia en el patrón de movimiento respiratorio. X Jornadas Complutenses, IX Congreso Nacional Investigación Alumnos Pregraduados en CC. De la Salud y XIV Congreso CC. Veterinarias y Biomédicas. Madrid, España. Universidad Complutense de Madrid

Waldeyer A, and Mayet A. 1987. Anatomie des Menschen: de Gruyter. 493 p.

Ward ME, Macklem PT. 1985. Kinematics of the chest wall. In: The Thorax. Roussos CJ, Macklem PT, ets. New York: Marcel Dekker Inc p 515-533

Ward ME, Ward JW, and Macklem PT. 1992. Analysis of human chest wall motion using a two-compartment rib cage model. Journal of Applied Physiology 72(4):1338-1347.

Weaver AA, Schoell SL, Stitzel JD. 2014. Morphometric analysis of variation in the ribs with age and sex. J Anat. 225:246-261

West JB. 1990. Respiratory physiology. The essentials. 4th ed. Baltimore: Williams & Wilkins.

West JB. 2012. Respiratory Physiology The Essentials, 9th edition ed. Philadelphia, Baltimore, New York, London, Buenos Aires, Hong Kong, Sydney, Tokyo: Wolters Kluwer, Lippincott Williams & Williams,

White TD, Black MT, Folkens TA, (Eds.) 2011. Human Osteology 3rd ed. Oxford, Academic Press.

Table 1. Regression of rib-pair shape on kinematic status and kinematic angles between rib pairs. Each angle is calculated between the kinematic trajectory of the pair of ribs in whose row the value is indicated and those in the row above.

rib pairs	% of explained variance	p-value	angle (degrees)	p-value
pair 1-2	13.14	**0.001**		
pair 2-3	14.73	**0.001**	18.91	**0.0000**
pair 3-4	12.64	**0.001**	12.87	**0.0000**
pair 4-5	9.12	**0.006**	11.31	**0.0000**
pair 5-6	6.95	**0.036**	13.72	**0.0000**
pair 6-7	5.88	0.061	14.57	**0.0000**
pair 7-8	5.06	0.114	12.25	**0.0000**
pair 8-9	4.71	0.128	11.88	**0.0001**
pair 9-10	4.62	0.137	13.51	**0.0001**

Table 2. Kinematic differences in centroid size (mm) and shape (Procrustes distance, Pd) between forced inspiration and forced expiration in the pulmonary thorax and the diaphragmatic thorax. (ns not significant).

units	Pulmonary Thorax	Diaphragmatic Thorax	t	p
Centroid size	12.62	34.47	-4.54	<0.0001
Procrustes distance	0.053	0.046	1.07	ns

Table 3. Relationships between functional size (*fs*) and functional shape (*fsh*) of the pulmonary thorax (PT) and diaphragmatic thorax (DT). Reduced major axis regression analyses (slopes, 95% confidence intervals), intercept, correlation coefficient, and p-value.

units	slope (95% C.I.)	intercept	r	p
Functional size: PT vs DT	0.35 (0.21-1.13)	0.47 (-25.19-4.52)	0.41	0.07
Functional shape: PT vs DT	0.99 (0.75-1.09)	0.007 (0.001-0.016)	0.95	0.0001
PT *fs* vs PT *fsh*	335.6 (191.8-422.9)	-5.34 (-20.03-6.385)	0.73	0.0002
DT *fs* vs PT *fsh*	946.22 (609.7-1097)	-9.27 (-20.03-6.385)	0.77	0.0002

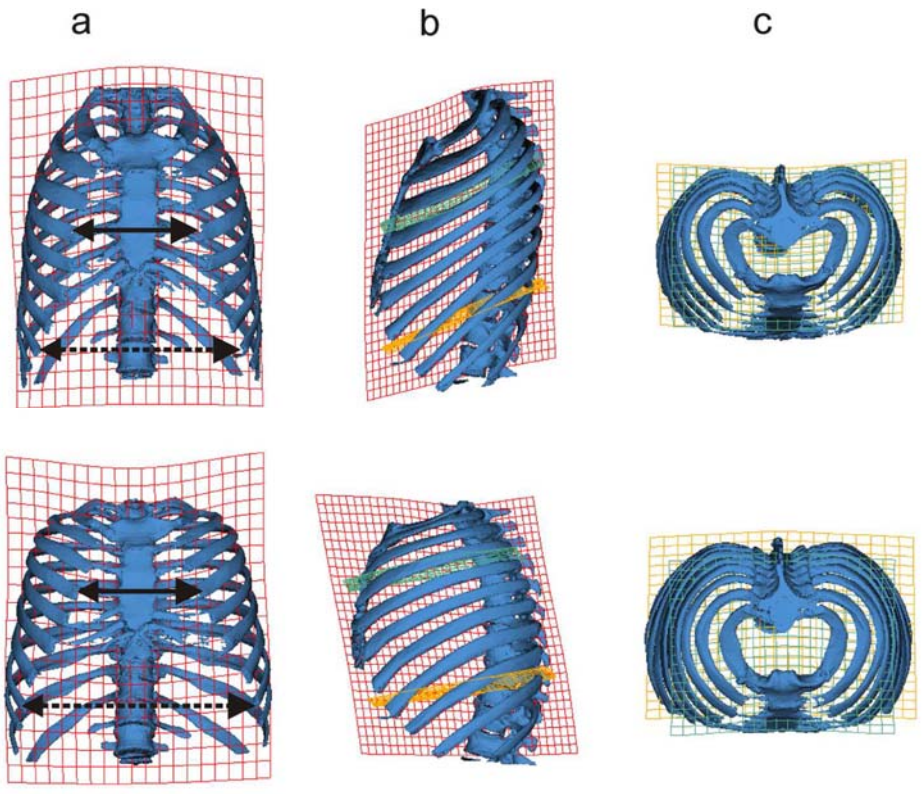

Figure 1. How the thorax changes shape during breathing. Upper row: forced expiration; lower row: forced inspiration; a, anterior; b, left lateral; c, superior axial views.

Grids are warped from the overall mean shape to the mean shapes at forced inspiration and forced expiration. In frontal view the red transformation grids are drawn through the centre of the ribcage, in lateral view the grids are drawn through the midsagittal plane. In axial view grids are drawn in the transverse plane at the level of the mid upper thorax (green grid) and mid lower thorax (orange grid). a) shows the relatively lower position of the lateral parts of the ribs which become elevated during inspiration. In addition, the lower thorax becomes mediolaterally wider relative to the upper, also shown by transformation grids in (c). The solid line and arrows show no change in width in the upper part of the thorax. The dashed line and arrows show medio-lateral expansion in the lower thorax during inspiration. Left lateral views (b) show a considerably more marked antero-posterior expansion of the upper than of the lower thorax. The cranial axial views also illustrate that the upper thorax in expiration (c) is shallower in the antero-posterior direction relative to the lower thorax, becoming relatively deeper during inspiration. Thus, the green transformation grid in the upper thorax is relatively shorter in FE than in FI, while the orange grid changes in its medio-lateral width, but not in its anteroposterior depth.

177x145mm (300 x 300 DPI)

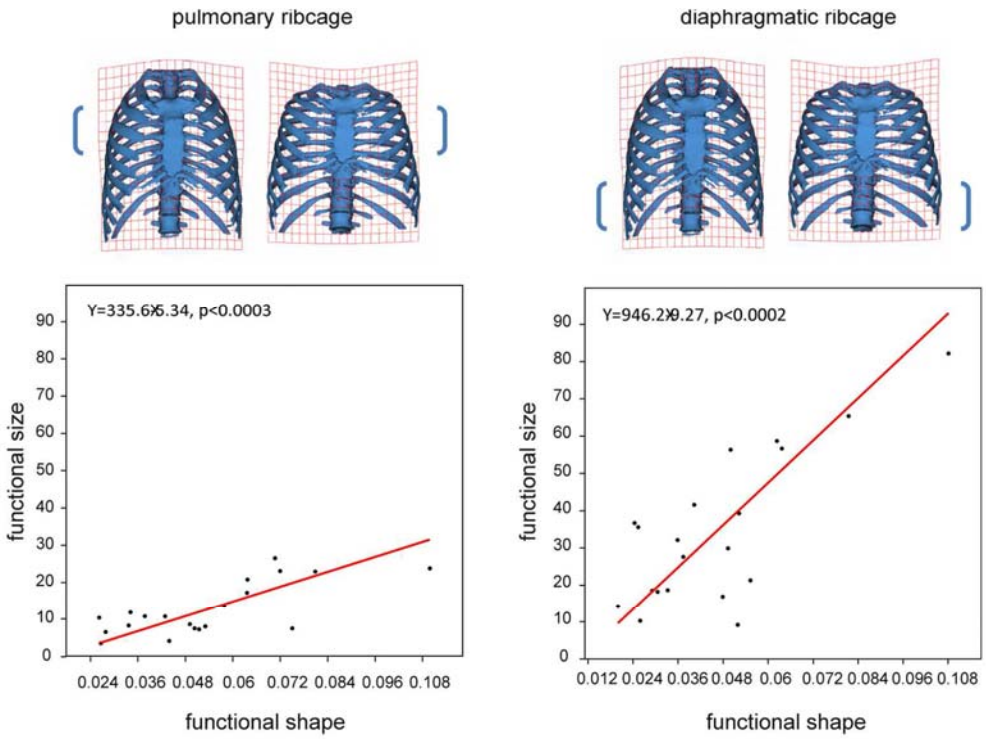

Figure 2. Functional size and shape changes of the pulmonary and diaphragmatic ribcage. The slope of the pulmonary ribcage is considerably smaller than that of the diaphragmatic ribcage. Therefore, within the lower thorax, less shape change is necessary to produce the same degree of size difference as in the upper thorax.
186x139mm (300 x 300 DPI)

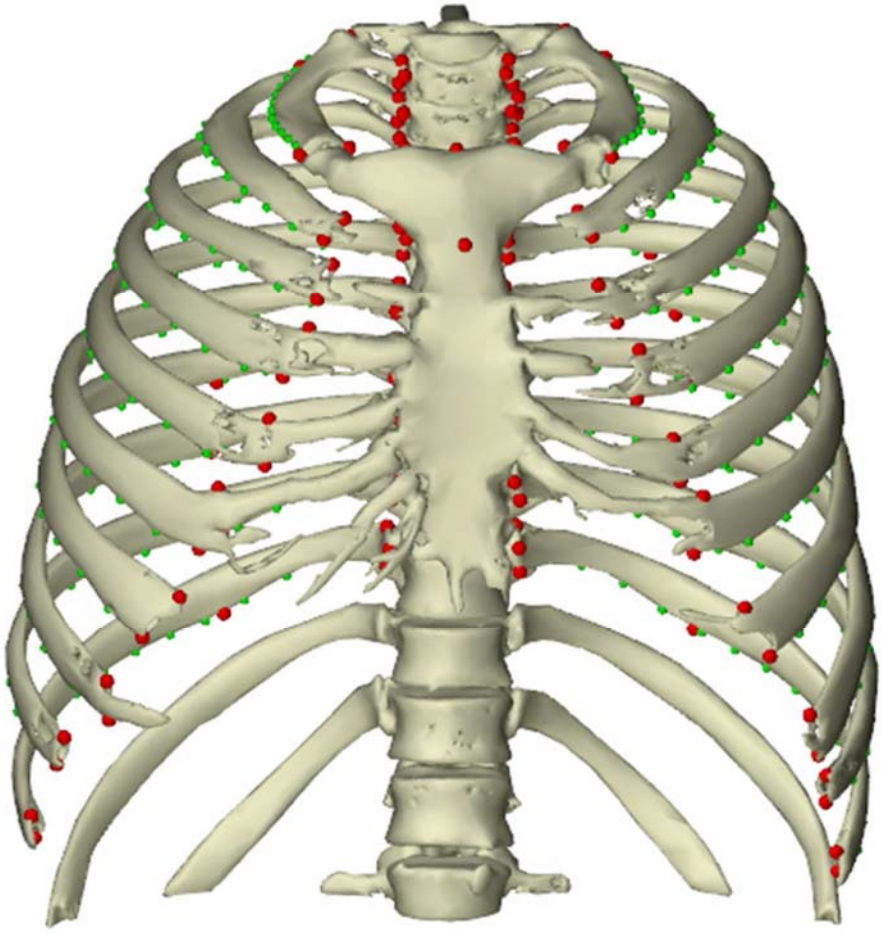

Supplementary Figure 1. This figure shows a 3D reconstruction of an adult thorax in forced inspiration (FI). The red dots mark anatomical landmarks, the green dots semilandmarks which characterize the 3D curvature of the ribs.
127x136mm (96 x 96 DPI)

Supplementary Figure 1. This figure shows a 3D reconstruction of an adult thorax in forced inspiration (FI). The red dots mark anatomical landmarks, the green dots semilandmarks which characterize the 3D curvature of the ribs.

Supplementary Movie 1. This movie shows the shape changes of the full thorax in frontal view during inspiration and expiration. Upper and lower thorax compartments are marked by green and orange thin-plate spline (TPS) grids and the kinematic changes of the full thorax is shown by the red frontal TPS grid transformation. The kinematic shape changes are magnified slightly (1.5x) for better visualization. Note the strong lateral elevation of the upper ribs and marked mediolateral widening of the lower ribs, which is absent in the upper thorax.